molecular pharmaceutics

ARTICLE

pubs.acs.org/molecularpharmaceutics

The Solubility−Permeability Interplay: Mechanistic Modeling and Predictive Application of the Impact of Micellar Solubilization on Intestinal Permeation

Jonathan M. Miller,[†] Avital Beig,[‡] Brian J. Krieg,[§] Robert A. Carr,[†] Thomas B. Borchardt,[†] Gregory E. Amidon,[§] Gordon L. Amidon,[§] and Arik Dahan*[,‡]

[†]Global Pharmaceutical Research and Development, Abbott Laboratories, Abbott Park, Illinois 60064, United States

[‡]Department of Clinical Pharmacology, School of Pharmacy, Faculty of Health Sciences, Ben-Gurion University of the Negev, Beer-Sheva 84105, Israel

[§]Department of Pharmaceutical Sciences, The University of Michigan College of Pharmacy, 428 Church Street, Ann Arbor Michigan 48109, United States

ABSTRACT: Surfactants are routinely employed to increase the apparent aqueous solubility of poorly soluble drugs. Yet the impact of micellar solubilization on the intestinal membrane permeability of a lipophilic drug is often overlooked and poorly understood. In this work, the interplay between the apparent solubility increase and intestinal membrane permeability decrease that exists when surfactants are used as drug solubility enhancers is described. A quasi-equilibrium mechanistic mass transport analysis was developed and employed to describe the effect of micellar solubilization by sodium taurocholate (STC) and sodium lauryl sulfate (SLS) on the intestinal membrane permeability of the lipophilic drug progesterone. The model considers the effects of micellar solubilization on both the membrane permeability (P_m) and the unstirred water layer (UWL) permeability (P_{aq}), to predict the overall effective permeability (P_{eff}) dependence on surfactant concentration (C_S). The analysis reveals that (1) the effective UWL thickness (h_{aq}) quickly decreases with increasing C_S above the critical micelle concentration (CMC), such that P_{aq} markedly increases with increasing C_S; (2) the free fraction of drug available for membrane permeation decreases with increasing C_S above CMC, such that P_m decreases with increasing C_S; and (3) P_{aq} increases and P_m decreases with increasing C_S above CMC, consequently the UWL is effectively shorted out and the overall P_{eff} tends toward membrane control with increasing C_S. The model enabled excellent quantitative prediction of the progesterone P_{eff} as a function of C_S in the rat jejunal perfusion model. This work demonstrates that a trade-off exists between micellar apparent solubility increase and permeability decrease that must be taken into account to strike the optimal solubility−permeability balance. The model presented in this work offers the formulation scientist a simple method for *a priori* prediction of this interplay, in order to maximize the overall oral absorption.

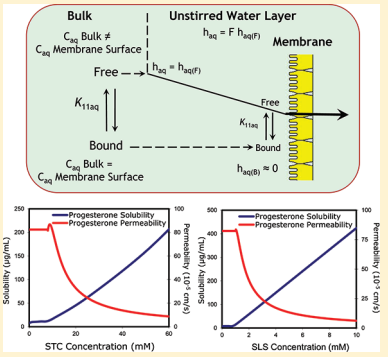

KEYWORDS: low-solubility drugs, surface active agents, solubility-permeability trade-off, drug transport analysis, intestinal permeation, oral drug absorption, surfactants, drug solubility, intestinal membrane permeability, sodium taurocholate, sodium lauryl sulfate, progesterone

INTRODUCTION

Advancements in drug discovery have led to drug candidates that are designed to hit more novel and sophisticated biological targets. This has resulted in chemical libraries that contain many more molecules with inherently higher molecular weight and lipophilicity. Consequently, an increasing number of water insoluble drug candidates are being selected for development.[1−3]

According to the Biopharmaceutics Classification System (BCS), the extent of oral absorption of a drug is governed by two primary factors: (1) the effective permeability across the intestinal mucosa and (2) the solubility and dissolution characteristics in the gastrointestinal (GI) milieu.[3−7] Since drugs must dissolve in the GI tract in order to be absorbed, compounds with inadequate aqueous solubility often suffer from limited oral absorption and bioavailability. The modern biopharmaceutical scientist must overcome these barriers via solubility enabling formulation technologies to improve the oral absorption of these poorly soluble drug candidates.[8−11]

Surfactants are often crucial for improving the apparent solubility and enabling the oral absorption of poorly soluble drugs. Endogenous surfactants such as sodium taurocholate (STC) are naturally present in the GI tract and play important roles in lipid digestion/absorption, as well as solubilization of lipophilic drugs. The use of artificial surfactants as excipients in the dosage form has long been a preferred approach to improve the apparent aqueous solubility of poorly soluble drugs.[12] Above the critical micelle

Received: April 11, 2011
Accepted: July 29, 2011
Revised: July 18, 2011
Published: July 29, 2011

ACS Publications © 2011 American Chemical Society

concentration (CMC), surfactants can incorporate drug into micelles, which can lead to extraordinary increases in the apparent solubility of lipophilic drugs. However, this micellar solubilization, which gives rise to this important apparent solubility enhancement, also results in decreased free fraction of drug. This can significantly decrease the amount of drug available for intestinal membrane permeation.[13−20]

Previous studies have shown that the use of surfactants may lead to increased, decreased, or unchanged membrane permeability.[13−18,20−25] For hydrophilic drugs with poor intestinal membrane permeability (e.g., BCS class III), surfactants can often increase intestinal membrane permeability. This may occur through the inhibition of efflux transporters and/or the disruption of membrane integrity to increase paracellular transport (e.g., tight junction opening, which may induce potentially toxic effects).[20−25] On the other hand, for lipophilic drugs with high transcellular membrane permeability (e.g., BCS class II), surfactants can decrease the free fraction of drug which results in decreased intestinal membrane permeability.[13−20]

In this work, we show that the effect of surfactant on the permeability of a lipophilic drug is due to the interplay between the apparent solubility increase and intestinal membrane permeability decrease that exists when surfactants are used as drug solubility enhancers. We have incorporated the various aspects of the solubility−permeability interplay as a whole, putting special emphasis on the effect of surfactant on unstirred water layer (UWL) and intestinal membrane permeability as well as diffusivity and viscosity. We have employed the single-pass rat jejunal perfusion as the permeability experimental model, since it has been proven to simulate well the real *in vivo* situation, including the UWL and the membrane permeability. This approach enabled us previously to reveal the solubility−permeability interplay in a cyclodextrin-based solubilization scenario.[19] Sodium taurocholate (STC) and sodium lauryl sulfate (SLS) were chosen as the model surfactants for this work, in order to cover both naturally occurring and solubility-enabling formulation scenarios. The model drug used in this work is the highly lipophilic, low-solubility, BCS class II drug progesterone, which is not known to be a substrate for transporters. Overall, this work provides an increased understanding of the underlying mechanisms that govern the effects of micellar solubilization on intestinal membrane transport, and enables the more efficient and intelligent use of solubility-enabling formulation strategies to facilitate oral absorption.

THEORY

Quasi-Equilibrium Analysis of the Effect of Surfactant on Membrane Permeability. The intrinsic membrane permeability of free drug ($P_{m(F)}$) in the absence of micelles (i.e., either no surfactant or below the CMC) can be written as[26]

$$P_{m(F)} = \frac{D_{m(F)}K_{m(F)}}{h_{m(F)}} \quad (1)$$

where $D_{m(F)}$ is the membrane diffusion coefficient of the free drug in the absence of micelles, $K_{m(F)}$ is the membrane/aqueous partition coefficient of drug in the absence of micelles, and $h_{m(F)}$ is the membrane thickness experienced by free drug in the absence of micelles.

Likewise, the apparent membrane permeability of the drug in the presence of micelles (P_m) can be written as

$$P_m = \frac{D_m K_m}{h_m} \quad (2)$$

where D_m is the apparent membrane diffusion coefficient of the drug in the presence of micelles and K_m is the apparent membrane/aqueous partition coefficient of the drug in the presence of micelles.

Surfactant micelles are generally not passively absorbed, so it can be assumed that only the free drug permeates the membrane such that $D_{m(F)} = D_m$ and that the presence of surfactant micelles does not affect the membrane thickness such that $h_{m(F)} = h_m$; eqs 1 and 2 can be combined to give

$$P_m = \frac{P_{m(F)}K_m}{K_{m(F)}} \quad (3)$$

$K_{m(F)}$ and K_m can be expressed as

$$K_{m(F)} = \frac{S_{m(F)}}{S_{aq(F)}} \quad (4)$$

$$K_m = \frac{S_m}{S_{aq}} \quad (5)$$

where $S_{m(F)}$ is the membrane solubility of the free drug, $S_{aq(F)}$ is the aqueous solubility of the free drug, S_m is the apparent membrane solubility of the drug in the presence of micelles, and S_{aq} is the apparent aqueous solubility of the drug in the presence of micelles.

Since surfactant micelles do not generally permeate into the intestinal membrane, it can be assumed that the presence of surfactant micelles does not affect the drug solubility in the membrane such that $S_{m(F)} = S_m$; eqs 3, 4, and 5 can be combined to give

$$P_m = \frac{P_{m(F)}S_{aq(F)}}{S_{aq}} \quad (6)$$

The dependence of drug apparent aqueous solubility on surfactant concentration (C_S) above the CMC can be written as[13]

$$S_{aq} = S_{aq(F)}(K_{11aq}C_S + 1) \quad (7)$$

where K_{11aq} is the aqueous association constant of the 1:1 drug:micelle complex.

Equations 6 and 7 can be combined to express the P_m dependence on C_S:

$$P_m = \frac{P_{m(F)}}{(K_{11aq}C_S + 1)} \quad (8)$$

Recognizing that above the CMC, the fraction of free drug (F) can be written as

$$F = \frac{S_{aq(F)}}{S_{aq}} = \frac{1}{K_{11aq}C_S + 1} \quad (9)$$

Equations 8 and 9 can be combined to express the P_m dependence on F:

$$P_m = P_{m(F)}F \quad (10)$$

The intrinsic permeability of the free drug through the unstirred aqueous boundary layer ($P_{aq(F)}$) in the absence of micelles (i.e., either no surfactant or below the CMC) can be written as[13,19]

$$P_{aq(F)} = \frac{D_{aq(F)}}{h_{aq(F)}} \quad (11)$$

where $D_{aq(F)}$ is the diffusion coefficient of the free drug through the unstirred aqueous boundary layer in the absence of micelles

and $h_{aq(F)}$ is the unstirred aqueous boundary layer thickness experienced by free drug in the absence of micelles.

Likewise, the apparent unstirred aqueous boundary layer permeability of the drug in the presence of micelles (P_{aq}) can be written as

$$P_{aq} = \frac{D_{aq}}{h_{aq}} \tag{12}$$

where D_{aq} is the apparent diffusion coefficient of the drug through the unstirred aqueous boundary layer in the presence of micelles and h_{aq} is the apparent unstirred aqueous boundary layer thickness in the presence of micelles.

Equations 11 and 12 can be combined to give

$$P_{aq} = \frac{P_{aq(F)} D_{aq} h_{aq(F)}}{D_{aq(F)} h_{aq}} \tag{13}$$

D_{aq} may be expressed as[13,19]

$$D_{aq} = FD_{aq(F)} + BD_{aq(B)} \tag{14}$$

Where B is the fraction of drug molecules bound to micelles ($B = 1 - F$) and $D_{aq(B)}$ is the aqueous diffusion coefficient of the drug−micelle complex.

Likewise, h_{aq} may be expressed as[19]

$$h_{aq} = Fh_{aq(F)} + Bh_{aq(B)} \tag{15}$$

where $h_{aq(B)}$ is the apparent unstirred aqueous boundary layer thickness experienced by the drug−micelle complex.

Equations 11, 13, 14 and 15 can be combined to show the dependence of P_{aq} on both free and micelle bound drug:

$$P_{aq} = \frac{(FD_{aq(F)} + BD_{aq(B)})}{(Fh_{aq(F)} + Bh_{aq(B)})} \tag{16}$$

Micellar association of progesterone facilitates the transport of drug directly to the membrane surface,[13,19] so it can be assumed that the unstirred aqueous boundary layer is no longer significant for the drug−micelle complex (i.e., $h_{aq(B)} = 0$ and $h_{aq} = Fh_{aq(F)}$). As such, eqs 9 and 16 can be combined to express the P_{aq} dependence on C_S:

$$P_{aq} = \frac{P_{aq(F)} D_{aq} (K_{11aq} C_S + 1)}{D_{aq(F)}} \tag{17}$$

Taking into account the membrane permeability as well as the unstirred aqueous boundary layer permeability on either side of the membrane, $P_{aq(1)}$ and $P_{aq(2)}$, the overall effective permeability (P_{eff}) of the drug can be written as[13,19]

$$P_{eff} = \frac{1}{\frac{1}{P_{aq(1)}} + \frac{1}{P_m} + \frac{1}{P_{aq(2)}}} \tag{18}$$

For simplicity, $P_{aq(2)}$ is assumed to have a negligible effect, such that $P_{aq(1)} = P_{aq}$, and eq 18 can be rewritten as

$$P_{eff} = \frac{1}{\frac{1}{P_{aq}} + \frac{1}{P_m}} \tag{19}$$

Thus, the overall P_{eff} dependence on C_S may be predicted via eq 19 wherein the P_m and P_{aq} dependence on C_S are predicted using eqs 8 and 17 with knowledge of $P_{m(F)}$, K_{11aq}, $P_{aq(F)}$, $D_{aq(F)}$, and D_{aq}.

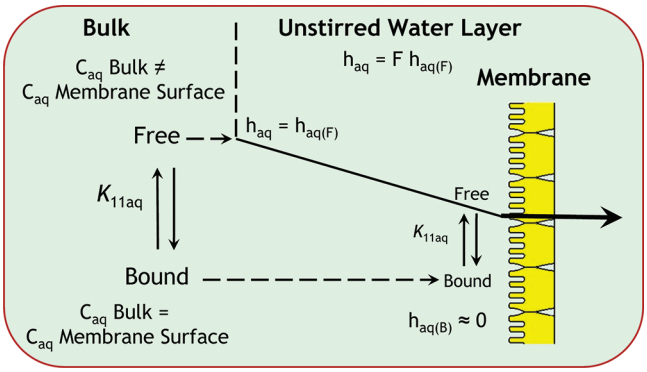

Figure 1. Schematic illustration of the quasi-equilibrium transport model through the unstirred water layer and the intestinal membrane.

Moreover, the drug concentration at the interface between the UWL and membrane ($C_{aqMembraneSurface}$) as a function of C_S can be calculated according to the following equation:[13,19]

$$\frac{C_{aqMembraneSurface}}{C_{aqBulk}} = \frac{P_{eff}}{P_m} \tag{20}$$

The assumptions nested in these analyses include the following: (1) quasi-equilibrium conditions; (2) only the free drug partitions and diffuses into the membrane, but not the drug: micelle complex, such that $S_{m(F)} = S_m$ and $D_{m(F)} = D_m$; (3) the presence of micelles does not affect the membrane thickness such that $h_{m(F)} = h_m$; and (4) only the free drug encounters a significant unstirred aqueous boundary layer thickness but the unstirred aqueous boundary layer thickness is negligible for the drug−micelle complex such that $h_{aq(B)} = 0$. A schematic illustration of the quasi-equilibrium transport model through the unstirred water layer and the intestinal membrane is presented in Figure 1.

MATERIALS AND METHODS

Materials. Progesterone, sodium lauryl sulfate (SLS), sodium taurocholate (STC), 2-(*N*-morpholino)ethanesulfonic (MES) acid, and phenol red were purchased from Sigma Chemical Co. (St. Louis, MO). KCl and NaCl were obtained from Fisher Scientific Inc. (Pittsburgh, PA). Acetonitrile and water (Acros Organics, Geel, Belgium) were HPLC grade. All other chemicals were of analytical reagent grade.

Solubility Determinations. Progesterone apparent solubility at increasing concentrations of SLS and STC was measured at 37 °C in triplicate. Aqueous solutions of SLS (0−10 mM) and STC (0−75 mM) were added to glass vials containing excess amounts of progesterone. The vials were tightly closed and placed in a shaking water bath at 37 °C and 100 rpm. Establishment of equilibrium was assured by comparison of samples after 24 and 48 h. Before sampling, the vials were centrifuged at 10,000 rpm for 10 min. Supernatant was carefully withdrawn from each test tube and immediately assayed for drug content by HPLC.

Viscosity Determinations. A Cannon-Ubbeholde semi-micro calibrated viscometer (Cannon Instrument Company) was used to measure the viscosity of the aqueous solution and the 95% sodium taurocholate surfactant solutions at the concentrations used for the dissolution experiments (Note: the concentrations used for the 99% sodium dodecyl sulfate solutions were confirmed to be too small to cause a change in viscosity with respect to the buffer solution). Calibration of the viscometer was

done according to USP (USP 32-NF 27 Chapter ⟨911⟩, 2009) using deionized water. Surfactant solutions were prepared the day of the viscosity measurements. The viscometer was filled and was vertically aligned in a water bath kept at 37 °C and equilibrated for 20 min. Solution kinematic viscosity was determined by USP ⟨911⟩ using the calibration constant.

Rotating Disk Dissolution Experiments. Effective diffusion coefficients (D_{eff}) of progesterone at increasing concentrations of SLS and STC were measured using the rotating disk dissolution method. Progesterone powder was compressed into a 1 cm diameter die using a Carver hydraulic press at 170 MPa compression force and dwell time of 2.5 min. Solutions SLS (0, 2.5, 5, 10 mM) and STC (0, 25, 50, 75 mM) in 10 mM MES buffer, pH 6.5, were prepared the day of the dissolution runs. The surfactants were added after the aqueous buffer was degassed using a vacuum aspirator. The rotating disk dissolution experiments were carried out in 75 mL of surfactant solution in a jacketed beaker maintained at 37 °C. The dissolution tests were run for 1 h at 100 rpm with 250 μL samples taken every ten minutes. After the 250 μL samples were taken, they were centrifuged at 10,000 rpm for 10 min to separate any solid particles, and progesterone concentration was then determined by HPLC. Also, 250 μL of fresh buffer with the appropriate surfactant concentration was added to the dissolution medium after sampling. The effective diffusion coefficient at each surfactant concentration was calculated using the Levich equation:[27]

$$D_{\text{eff}} = \left(\left(\frac{J}{\nu^{-1/6} w^{1/2} S_{\text{aq}}}\right)/0.62\right)^{3/2} \tag{21}$$

where J is the dissolution rate, w is the rotation speed, and ν is the kinematic viscosity at a given surfactant concentration.

Rat Jejunal Perfusion. All animal experiments were conducted using protocols approved by the Ben-Gurion University of the Negev Animal Use and Care Committee (Protocol IL-60-11-2010) and the University Committee of Use and Care of Animals (UCUCA) of the University of Michigan (Protocol 8405). Animals were housed and handled according to the Ben-Gurion University of the Negev and the University of Michigan Units for Laboratory Animal Medicine guidelines. Male albino Wistar rats (Harlan, Israel) weighing 250−280 g were used for all perfusion studies. Prior to each experiment, the rats were fasted overnight (12−18 h) with free access to water. Animals were randomly assigned to the different experimental groups.

The procedure for the *in situ* single-pass intestinal perfusion followed previously published reports.[28−30] Briefly, rats were anesthetized with an intramuscular injection of 1 mL/kg of ketamine−xylazine solution (9%:1%, respectively) and placed on a heated surface maintained at 37 °C (Harvard Apparatus Inc., Holliston, MA). The abdomen was opened by a midline incision of 3−4 cm. A proximal jejunal segment (3 ± 1 cm average distance of the inlet from the ligament of Treitz) of approximately 10 cm was carefully exposed and cannulated on two ends with flexible PVC tubing (2.29 mm i.d., inlet tube 40 cm, outlet tube 20 cm, Fisher Scientific Inc., Pittsburgh, PA). Care was taken to avoid disturbance of the circulatory system, and the exposed segment was kept moist with 37 °C normal saline solution. The perfusate buffer consisted of 10 mM MES buffer, pH 6.5, 135 mM NaCl, 5 mM KCl, and 0.1 mg/mL phenol red. Phenol red was added to the perfusion buffer as a nonabsorbable marker for measuring water flux. Perfusate solutions of progesterone were prepared at SLS concentrations of 0, 0.5, 2.5, 5, and 10 mM and STC concentrations of 0, 2.5, 10, 25, and 50 mM. The progesterone concentration was made up at 75% the maximum apparent solubility in each surfactant solution in order to keep thermodynamic activity constant across all perfusate solutions. All perfusate solutions were incubated in a 37 °C water bath to maintain temperature and were pumped through the intestinal segment (Watson Marlow Pumps 323S, Watson- Marlow Bredel Inc., Wilmington, MA). The isolated segment was first rinsed with blank perfusion buffer, pH 6.5 at a flow rate of 0.5 mL/min in order to clean out any residual debris. At the start of the study, the test solutions were perfused through the intestinal segment at a flow rate of 0.2 mL/min. The perfusion buffer was first perfused for 1 h, in order to ensure steady state conditions (as also assessed by the inlet over outlet concentration ratio of phenol red which approaches 1 at steady state). After reaching steady state, samples were taken in 10 min intervals for one hour (10, 20, 30, 40, 50, and 60 min). All samples, including perfusion samples at different time points, original drug solution, and inlet solution taken at the exit of the syringe, were immediately assayed by HPLC. Following the termination of the experiment, the length of each perfused jejunal segment was accurately measured.

The net water flux in the single-pass rat jejunal perfusion studies, resulting from water absorption in the intestinal segment, was determined by measurement of phenol red, a nonabsorbed, nonmetabolized marker. The measured C_{out}/C_{in} ratio was corrected for water transport according to the following equation:

$$\frac{C'_{\text{out}}}{C'_{\text{in}}} = \frac{C_{\text{out}}}{C_{\text{in}}} \times \frac{C_{\text{inPhenolRed}}}{C_{\text{outPhenolRed}}} \tag{22}$$

where C_{out} is the concentration of progesterone in the outlet sample, C_{in} is the concentration of progesterone in the inlet sample, $C_{inPhenolRed}$ is the concentration of phenol red in the inlet sample, and $C_{outPhenolRed}$ is the concentration of phenol red in the outlet sample. The effective permeability (P_{eff}) through the rat gut wall in the single-pass intestinal perfusion studies was determined assuming the "plug flow" model expressed in the following equation:[31,32]

$$P_{\text{eff}} = \frac{-Q \ln(C'_{\text{out}}/C'_{\text{in}})}{2\pi RL} \tag{23}$$

where Q is the perfusion buffer flow rate, C'_{out}/C'_{in} is the ratio of the outlet concentration and the inlet or starting concentration of the tested drug that has been adjusted for water transport via eq 22, R is the radius of the intestinal segment (set to 0.2 cm), and L is the length of the intestinal segment.

High Performance Liquid Chromatography (HPLC). HPLC experiments were performed on an Agilent Technologies (Palo Alto, CA) HPLC 1100 equipped with photodiode array detector and ChemStation for LC 3D software. Progesterone was assayed using an Agilent (Palo Alto, CA) 150 mm × 4.6 mm XDB-C_{18} column with 5 μm particle size. The detection wavelength was 242 nm. The mobile phase consisted of 30:70 (v:v) 0.1% trifluoroacetic acid in water:0.1% trifluoroacetic acid in acetonitrile and was pumped at a flow rate of 1.0 mL/min. Injection volumes for all HPLC analyses ranged from 5 to 100 μL.

Statistical Analysis. All *in vitro* experiments were performed in triplicate (unless stated otherwise), and all animal experiments were $n = 4$. Values are expressed as the mean ± the standard deviation (SD). To determine statistically significant differences among the experimental groups, the nonparametric Kruskal−Wallis test was used for multiple comparisons, and the two-tailed nonparametric

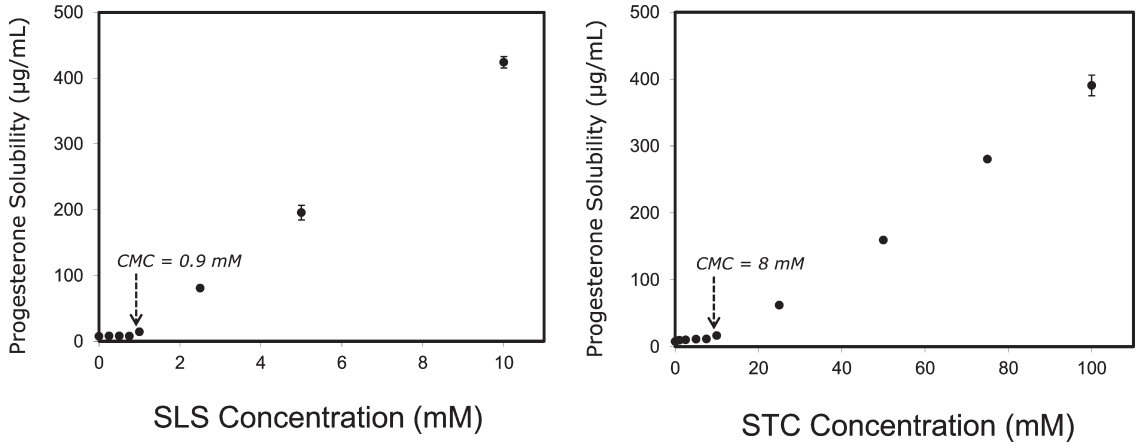

Figure 2. Apparent solubility of progesterone as a function of increasing SLS (left panel) and STC (right panel) concentration in MES buffer pH 6.5 at 37 °C.

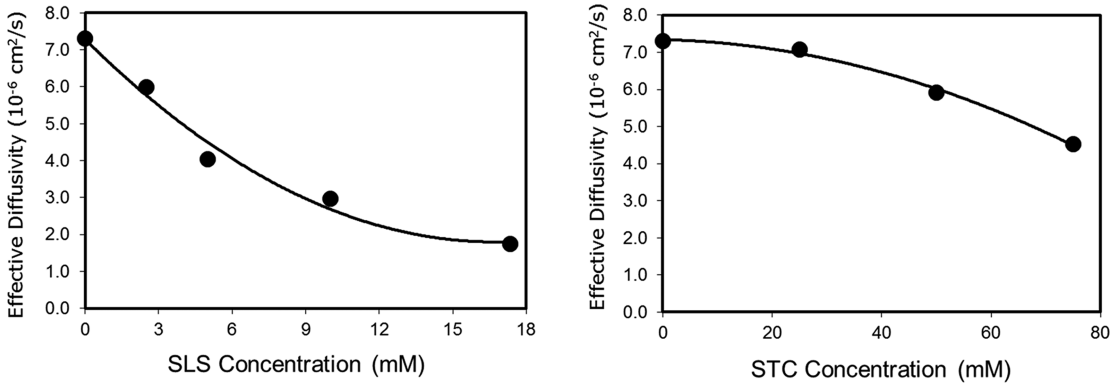

Figure 3. Effective diffusivity of progesterone as a function of increasing SLS (left panel) and STC (right panel) concentration in MES buffer pH 6.5 at 37 °C, determined using the rotating disk method.

Mann−Whitney *U*-test for two-group comparison where appropriate. A p value of less than 0.05 was termed significant.

RESULTS

Effect of SLS and STC on Progesterone Solubility. Progesterone apparent aqueous solubility as a function of SLS and STC concentration is presented in Figure 2. In both systems, the apparent solubility of progesterone remained constant below CMC and increased linearly ($R^2 > 0.99$) above CMC such that apparent CMC values of 0.9 mM for SLS and 8 mM for STC were readily approximated from the apparent solubility data. Association constants of 4310 M^{-1} for progesterone in SLS and 528 M^{-1} for progesterone in STC were determined from the apparent solubility data via eq 7.

Effect of SLS and STC on Progesterone Diffusivity. Diffusion coefficients of progesterone as a function of SLS and STC concentration were measured using the rotating disk method. In both the STC and the SLS systems, decreased progesterone diffusivity was observed with increasing surfactant levels (Figure 3). Solution viscosity increased minimally (approximately 7×10^{-3} to 8×10^{-3} cm^2/s) with increasing concentration of SLS (up to 15 mM) and STC (up to 75 mM), indicating that the decrease in apparent diffusivity of progesterone was not caused by increased solution viscosity, rather was predominantly due to micellar complexation.

Effect of SLS and STC on Progesterone Rat Jejunal Permeability. Progesterone permeability in the presence of increasing SLS and STC concentration was evaluated in the rat jejunal perfusion assay. Figure 4 shows the average P_{eff} of progesterone across rat jejunal segments with increasing surfactant concentrations. In the absence of surfactant, progesterone showed high permeability (82.4×10^{-5} cm/s) across rat jejunum. At surfactant concentrations below CMC, progesterone P_{eff} did not change in either surfactant system. However, the P_{eff} of progesterone decreased markedly with increasing SLS and STC concentrations above CMC (Figure 4). Progesterone P_{eff} decreased 2.1-, 4.6-, and 9.4-fold in the presence of 2.5, 5, and 10 mM SLS, respectively. Likewise, progesterone P_{eff} decreased 1.1-, 3.5-, and 6.7-fold in the presence of 10, 25, and 50 mM STC, respectively.

Figure 5 compares the predicted P_{eff} of progesterone as a function of SLS and STC concentration to the experimentally observed P_{eff} values. The predicted lines for P_m, P_{aq}, and P_{eff} were calculated via eqs 8, 17, and 19, respectively. The experimental parameters used in the calculations were the K_{11aq} values and effective diffusion coefficients of progesterone as a function of surfactant concentration in the SLS and STC systems (Figures 2 and 3). The experimental value for progesterone rat jejunal $P_{m(F)}$ of 250×10^{-5} cm/s used in the calculations was previously estimated by determining the P_{eff} of progesterone at increasing perfusate flow rates.[33] The value of $P_{aq(F)}$ used in the predictions was calculated according to eq 19 from the experimental values of

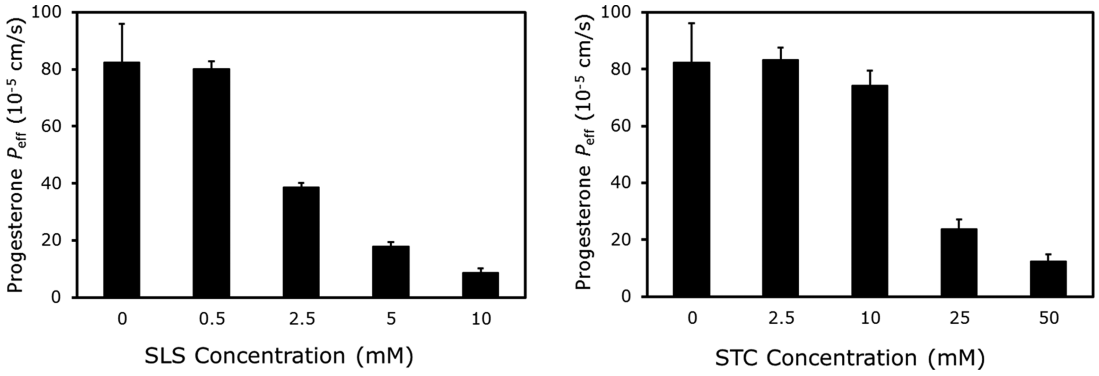

Figure 4. Effective permeability (P_{eff}, cm/s) of progesterone as a function of increasing SLS (left panel) and STC (right panel) concentration in the single-pass rat jejunal perfusion model.

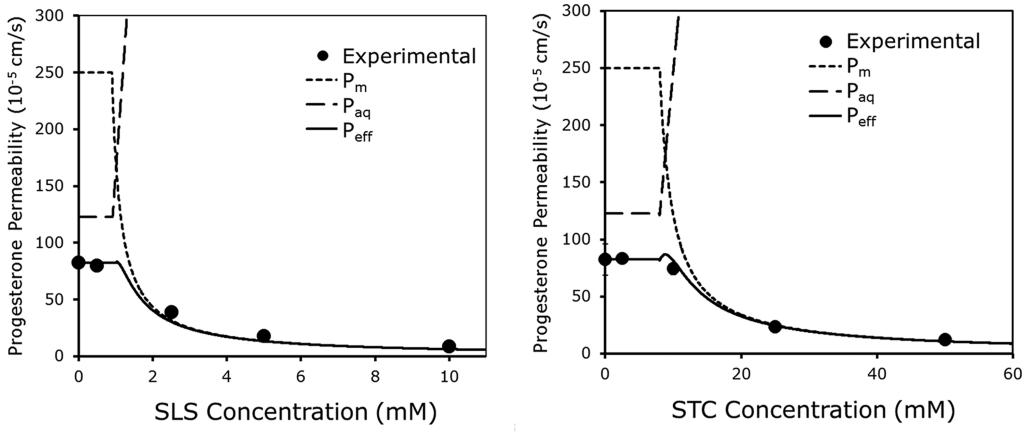

Figure 5. Permeability of progesterone as a function of SLS (left panel) and STC (right panel) concentration in the rat jejunal perfusion model. The theoretical lines were calculated via eq 8 (P_m), eq 17 (P_{aq}), and eq 19 (P_{eff}).

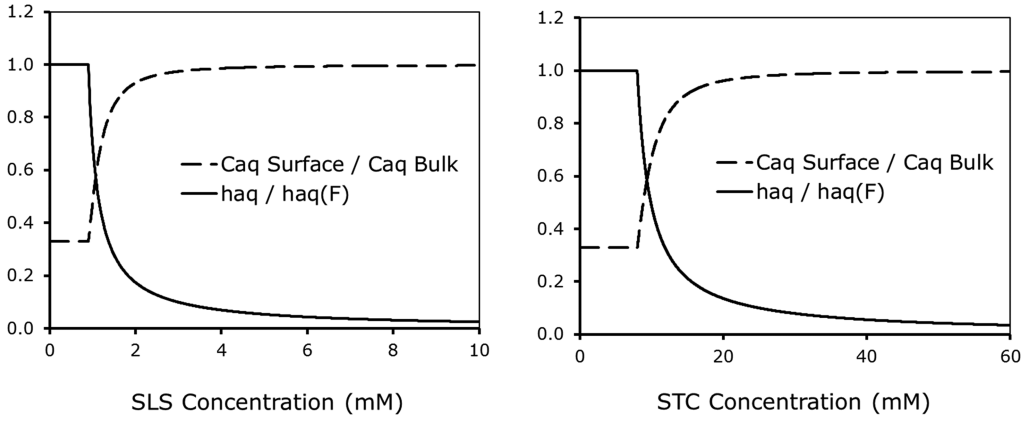

Figure 6. Theoretical membrane surface to bulk concentration ratio ($C_{aqSurface}/C_{aqBulk}$) and apparent (in presence of surfactant) to free drug aqueous boundary layer thickness ratio ($h_{aq}/h_{aq(F)}$) of progesterone as a function of SLS (left panel) and STC (right panel) concentration in the rat jejunal perfusion model, calculated according to eqs 15 and 20.

$P_{m(F)}$ and the P_{eff} of progesterone determined in the absence of surfactant (82.4×10^{-5} cm/s). Excellent agreement was obtained between the experimental and predicted progesterone P_{eff} values as a function of surfactant concentration in both the SLS and STC systems (Figure 5).

Figure 6 shows the theoretical membrane surface to bulk concentration ratio ($C_{aqSurface}/C_{aqBulk}$) and apparent (in presence of surfactant) to free drug aqueous boundary layer thickness ratio ($h_{aq}/h_{aq(F)}$) of progesterone as a function of SLS and STC concentration in the rat jejunal perfusion model. The predicted curves were calculated according to eqs 15 and 20. $C_{aqSurface}/C_{aqBulk}$ increases to approach 1 and $h_{aq}/h_{aq(F)}$ decreases to approach 0 with increasing surfactant concentration in both systems.

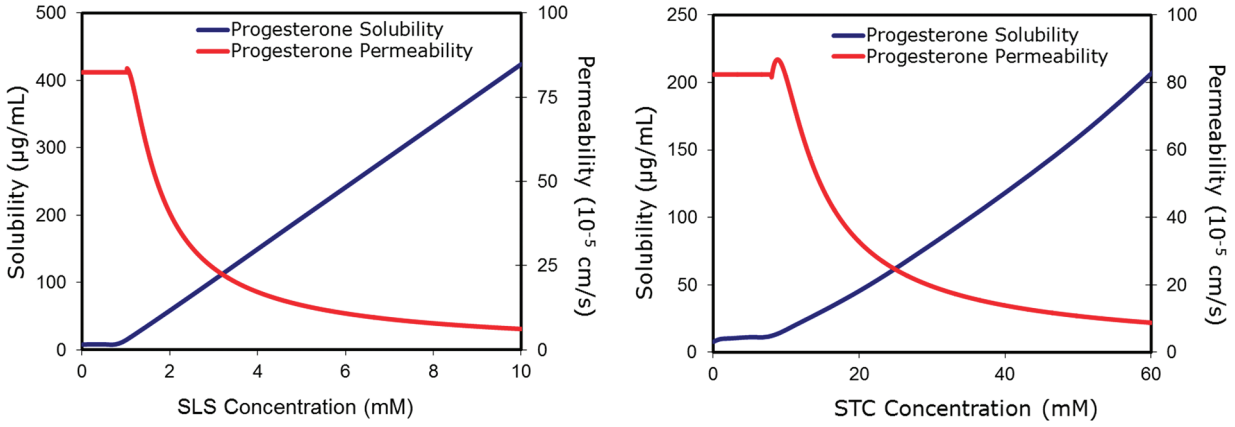

Figure 7. The effects of SLS (left panel) and STC (right panel) on progesterone apparent aqueous solubility and intestinal permeability based on the theoretical quasi-equilibrium transport model developed in this work.

Figure 7 illustrates the effects of SLS and STC on progesterone apparent aqueous solubility and intestinal permeability based on the theoretical quasi-equilibrium transport analysis developed in this work. This figure visibly illustrates the opposing effects a surfactant-based formulation may have on the apparent solubility and intestinal permeability.

DISCUSSION

In this research, we describe the interplay between the apparent solubility increase and intestinal membrane permeability decrease that exists when surfactants are used as drug apparent solubility enhancers. These opposing effects on apparent solubility and permeability must be taken into account in order to fully understand the impact on the overall fraction of drug absorbed when surfactants are employed to enhance the oral exposure of a poorly soluble drug. We offer a quantitative model that may be used to understand this solubility−permeability interplay, and predict *a priori* the trade-off that occurs between apparent solubility increase and intestinal permeability decrease when surfactants are used as pharmaceutical solubilizers.

Micellar complexation between progesterone and the surfactants results in substantially enhanced apparent aqueous solubility of the drug with increasing concentrations of SLS and STC above their apparent CMC values of 0.9 and 8 mM, respectively (Figure 2). This type of apparent solubility enhancement demonstrates the utility of surfactants for enabling the oral exposure of poorly soluble drugs, both through naturally occurring surfactants (e.g., STC) that are present *in vivo* and synthetic surfactants (e.g., SLS) which may be incorporated into the dosage form. However, the relatively high binding constants of 4310 M^{-1} for progesterone in SLS and 528 M^{-1} for progesterone in STC which give rise to this important apparent solubility enhancement also result in decreased free fraction of progesterone with increasing surfactant concentration above CMC. This decreased fraction of free drug can significantly decrease the amount of drug available for intestinal membrane permeation, as was observed in these studies.

The effective diffusion coefficient of progesterone decreased with increasing surfactant concentration in both the STC and the SLS systems (Figure 3). This is consistent with slower diffusivity expected for drug inside micelle vs free drug. A more marked decrease in effective diffusivity was observed for progesterone in SLS as compared to STC over the concentration ranges studied. This may be attributed to the significantly higher K_{11aq} for progesterone in SLS vs STC. The decrease in progesterone effective diffusivity with increasing surfactant concentration above CMC contributes to a slight decrease in the aqueous boundary layer permeability as expressed in eqs 12 and 18. However, this effect is largely negligible in comparison to the effect of the shrinking h_{aq} with increasing micellar solubilization of progesterone, which leads to a marked increase in P_{aq} with increasing SLS and STC concentrations above CMC (Figure 5). This may be explained by the micellar complexation of progesterone, as the UWL is only experienced by the free drug and is effectively eliminated for the progesterone−micelle complex (i.e., $h_{aq(B)} = 0$), such that the effective thickness of the boundary layer decreases with decreasing free fraction of progesterone (i.e., $h_{aq} = Fh_{aq(F)}$). At the same time, P_m remains constant below CMC, but then rapidly decreases with increasing surfactant concentration above CMC (Figure 5). This may also be attributed to the decrease in the amount of free drug available for membrane permeation with increasing surfactant concentration above CMC, as described in eqs 8 and 10.

Figure 5 contains the overall predicted P_{eff} as a function of SLS and STC concentration in the rat intestinal perfusion model. The predicted P_{eff} was calculated via eq 20, using the predicted values of P_{aq} and P_m as a function of surfactant concentration. Excellent agreement was obtained between the experimental and predicted progesterone P_{eff} values in both surfactant systems at all concentrations tested. The overall P_{eff} of progesterone stayed relatively unchanged at surfactant concentrations below CMC. This is because, at surfactant concentrations below CMC, progesterone is not incorporated into micelles and the overall P_{eff} remains limited by the UWL. This agrees with previous reports that have shown progesterone permeability to be limited by the aqueous boundary layer in the rat intestinal perfusion model.[19,33,34] Just beyond the CMC, the overall P_{eff} increases slightly, reaching a maximum around the point at which P_m and P_{aq} are essentially equal. Around this point, the overall P_{eff} is transitioning from being UWL to membrane controlled. As surfactant concentration increases further above the CMC, the rapidly decreasing effective h_{aq} causes P_{aq} to markedly increase, such that the UWL is quickly eliminated and the overall P_{eff} decreases and becomes membrane controlled (i.e., $P_{eff} \approx P_m$).

As shown in Figure 6, the progesterone concentration at the membrane surface gradually increases and becomes equal to bulk

as surfactant concentration increases, such that $h_{aq}/h_{aq(F)}$ decreases and approaches 0 with increasing SLS and STC concentration above CMC. In this way, micellar association of progesterone effectively shorts out the UWL by facilitating the transport of drug to the membrane surface such that $C_{aqMembraneSurface} \approx C_{aqBulk}$ with increasing surfactant concentration, and permeation across the intestinal membrane becomes rate limiting.[13,19] This also corroborates with and mechanistically explains the recent proposition by Yano et al. that micellar solubilization by surfactant enables the more direct partitioning of drug from micelle to the intestinal membrane.[20]

It should be emphasized that the effective thickness of the boundary layer in this model is defined as the distance from the intestinal membrane surface to the point at which drug concentration in the aqueous milieu becomes constant and equal to bulk. It is important to differentiate this thickness from that of the hydrodynamic boundary layer thickness, which is the distance from the intestinal membrane surface to the point at which the fluid hydrodynamics (i.e., mixing) become constant and equal to bulk. The hydrodynamic boundary layer thickness is fixed under set hydrodynamic conditions (as in this study) whereas the concentration boundary layer thickness may change depending on the length of the concentration gradient. Indeed, when $C_{aqMembraneSurface} \approx C_{aqBulk}$, there is no longer a concentration gradient, and hence there is no effective UWL thickness. In this way, the h_{aq} is essentially shrinking with increasing surfactant concentration, as shown in Figure 6. The shrinking effective h_{aq} also results directly from the decrease in free fraction of drug with increasing SLS and STC concentration. Indeed, the UWL thickness experienced by the free drug remains constant with increasing surfactant concentration. However, since the free fraction of drug decreases with increasing surfactant concentration above CMC and micellized drug does not experience a UWL thickness (i.e., $h_{aq(B)} = 0$), the overall effective UWL thickness decreased as bound fraction increases and free fraction decreases (i.e., $h_{aq} = Fh_{aq(F)}$).

It is interesting to consider the solubility−permeability interplay in the context of the surfactant concentration ranges that may be encountered *in vivo*. Bile salt concentrations in the GI lumen have been reported to be in the range of 3−5 mM in fasted state and 15−20 mM in fed state.[11,18,35,36] Accordingly, for STC, the surfactant concentration in fasted state would be expected to be well below CMC, leading to essentially no effect on the apparent solubility nor permeability (Figure 7). Conversely, in the fed state, STC concentrations would be well above CMC, resulting in a significant decrease in apparent permeability along with the increase in apparent solubility and dissolution rate. For SLS, the maximum amount used in a current oral dosage form is about 52 mg according to the FDA inactive ingredients guide. Assuming 100−250 mL GI fluid volume,[36] this would result in SLS concentrations of 0.7−1.8 mM in the actual *in vivo* situation. As with STC, this range may lead to SLS concentrations below or above CMC, such that the solubility−permeability interplay may or may not actually play a role in the true *in vivo* situation. It is also worth noting that, for preclinical formulations used to drive exposures in toxicological/efficacy evaluations, even higher concentrations of SLS may be used, which would certainly result in significant effects on both apparent solubility and permeability.

CONCLUSIONS

In this work we demonstrate the trade-off that exists between apparent solubility increase and permeability decrease that governs the overall fraction of dose absorbed, when taking the micellar solubilization approach. Given these opposing effects, both apparent solubility and permeability considerations must be taken into account, to strike the optimal balance in order to maximize overall absorption. The quasi-equilibrium mass transport analysis developed in this work could successfully predict the P_{eff} dependence on surfactant concentration. The insights revealed in this work offer a more efficient and intelligent use of surfactants in oral drug product formulation development.

AUTHOR INFORMATION

Corresponding Author

*Department of Clinical Pharmacology, School of Pharmacy, Faculty of Health Sciences, Ben-Gurion University of the Negev, P.O. Box 653, Beer-Sheva 84105, Israel. E-mail: arikd@bgu.ac.il. Tel: +972-8-6479483. Fax: +972-8-6479303.

ACKNOWLEDGMENT

This work was supported by a research grant from Abbott Laboratories.

REFERENCES

(1) Lipinski, C. A. Drug-Like Properties and the Causes of Poor Solubility and Poor Permeability. *J. Pharmacol. Toxicol. Methods* **2001**, *44*, 235–249.

(2) Van de Waterbeemd, H.; Smith, D. A.; Beaumont, K.; Walker, D. K. Property-Based Design: Optimization of Drug Absorption and Pharmacokinetics. *J. Med. Chem.* **2001**, *44*, 1313–1333.

(3) Amidon, G. L.; Lennernaes, H.; Shah, V. P.; Crison, J. R. A Theoretical Basis for a Biopharmaceutic Drug Classification: The Correlation of In-Vitro Drug Product Dissolution and In-Vivo Bioavailability. *Pharm. Res.* **1995**, *12*, 413–420.

(4) Lobenberg, R.; Amidon, G. L. Modern Bioavailability, Bioequivalence and Biopharmaceutics Classification System. New Scientific Approaches to International Regulatory Standards. *Eur. J. Pharm. Biopharm.* **2000**, *50*, 3–12.

(5) Martinez, M. N.; Amidon, G.L. A Mechanistic Approach to Understanding the Factors Affecting Drug Absorption: A Review of Fundamentals. *J. Clin. Pharmacol.* **2002**, *42* (6), 620–643.

(6) Yu, L. X.; Amidon, G. L.; Polli, J. E.; Zhao, H.; Mehta, M. U.; Conner, D. P.; Shah, V. P.; Lesko, L. J.; Chen, M.; Lee, V. H. L.; Hussain, A. S. Biopharmaceutics Classification System: The Scientific Basis for Biowaiver Extensions. *Pharm. Res.* **2002**, *19*, 921–925.

(7) Dahan, A.; Miller, J. M.; Amidon, G. L. Prediction of Solubility and Permeability Class Membership: Provisional BCS Classification of the World's Top Oral Drugs. *AAPS J.* **2009**, *11* (4), 740–746.

(8) Dahan, A.; Amidon, G. L. Gastrointestinal Dissolution and Absorption of Class II Drugs. In *Drug Bioavailability: Estimation of Solubility, Permeability, Absorption and Bioavailability*, 2nd ed.; van de Waterbeemd, H., Testa, B., Eds.; Methods and Principles in Medicinal Chemistry; Wiley-VCH Verlag GmbH & Co. KGaA: 2009; Vol. 40, pp 33−51.

(9) Dahan, A.; Hoffman, A. Enhanced Gastrointestinal Absorption of Lipophilic Drugs. In *Enhancement in Drug Delivery*; Touitou, E., Barry, B. W., Eds.; CRC Press LLC: Boca Raton, 2007; pp 111−131.

(10) Gao, Y.; Carr, R. A.; Spence, J. K.; Wang, W. W.; Turner, T. M.; Lipari, J. M.; Miller, J. M. A pH-Dilution Method for Estimation of Formulation Dependent Drug Solubility Along the Gastrointestinal Tract: Application to Physiologically Based Pharmacokinetic Modeling. *Mol. Pharmaceutics* **2010**, *7*, 1516–1526.

(11) Dahan, A.; Hoffman, A. Rationalizing the selection of oral lipid based drug delivery systems by an in vitro dynamic lipolysis model for improved oral bioavailability of poorly water soluble drugs. *J. Controlled Release* **2008**, *129* (1), 1–10.

(12) Liu, R.; Sadrzadeh, N.; Constantinides, P. Micellization and Drug Solubility Enhancement. In *Water Insoluble Drug Formulation*; Liu, R., Ed.; CRC Press: Boca Raton, 2000; pp 213−341.

(13) Amidon, G. E.; Higuchi, W. I.; Ho, N. F. H. Theoretical and Experimental Studies of Transport of Micelle-Solubilized Solutes. *J. Pharm. Sci.* **1982**, *71*, 77–84.

(14) Poelma, F. G. J.; Breaes, R.; Tukker, J. J. Intestinal absorption of drugs. III. The influence of taurocholate on the disappearance kinetics of hydrophilic and lipophilic drugs from the small intestine of the rat. *Pharm. Res.* **1990**, *7* (4), 392–397.

(15) Poelma, F. G. J.; Breas, R.; Tukker, J. J.; Crommelin, D. J. A. Intestinal absorption of drugs. The influence of mixed micelles on the disappearance kinetics of drugs from the small intestine of the rat. *J. Pharm. Pharmacol.* **1991**, *43* (5), 317–324.

(16) Katneni, K.; Charman, S. A.; Porter, C. J. H. Permeability assessment of poorly water-soluble compounds under solubilizing conditions: the reciprocal permeability approach. *J. Pharm. Sci.* **2006**, *95* (10), 2170–2185.

(17) Katneni, K.; Charman, S. A.; Porter, C. J. H. Impact of cremophor-EL and polysorbate-80 on digoxin permeability across rat jejunum: delineation of thermodynamic and transporter related events using the reciprocal permeability approach. *J. Pharm. Sci.* **2007**, *96* (2), 280–293.

(18) Dahan, A.; Hoffman, A. The effect of different lipid based formulations on the oral absorption of lipophilic drugs: the ability of in vitro lipolysis and consecutive ex vivo intestinal permeability data to predict in vivo bioavailability in rats. *Eur. J. Pharm. Biopharm.* **2007**, *67* (1), 96–105.

(19) Dahan, A.; Miller, J. M.; Hoffman, A.; Amidon, G. E.; Amidon, G. L. The Solubility-Permeability Interplay in Using Cyclodextrins as Pharmaceutical Solubilizers: Mechanistic Modeling and Application to Progesterone. *J. Pharm. Sci.* **2010**, *99* (6), 2739–2749.

(20) Yano, K.; Masaoka, Y.; Kataoka, M.; Sakuma, S.; Yamashita, S. Mechanisms of membrane transport of poorly soluble drugs: Role of micelles in oral absorption processes. *J. Pharm. Sci.* **2010**, *99* (3), 1336–1345.

(21) Nerurkar, M. M.; Ho, N. F. H.; Burton, P. S.; Vidmar, T. J.; Borchardt, R. T. Mechanistic roles of neutral surfactants on concurrent polarized and passive membrane transport of a model peptide in Caco-2 cells. *J. Pharm. Sci.* **1997**, *86* (7), 813–821.

(22) Mudra, D. R.; Borchardt, R. T. Absorption barriers in the rat intestinal mucosa: 1. application of an in situ perfusion model to simultaneously assess drug permeation and metabolism. *J. Pharm. Sci.* **2010**, *99* (2), 982–998.

(23) Mudra, D. R.; Borchardt, R. T. Absorption barriers in the rat intestinal mucosa. 3: Effects of polyethoxylated solubilizing agents on drug permeation and metabolism. *J. Pharm. Sci.* **2010**, *99* (2), 1016–1027.

(24) Mudra, D. R.; Jin, J. Y.; Borchardt, R. T. Absorption barriers in the rat intestinal mucosa: 2. Application of physiologically based mathematical models to quantify mechanisms of drug permeation and metabolism. *J. Pharm. Sci.* **2010**, *99* (2), 999–1015.

(25) Rege, B. D.; Kao, J. P. Y.; Polli, J. E. Effects of nonionic surfactants on membrane transporters in Caco-2 cell monolayers. *Eur. J. Pharm. Sci.* **2002**, *16* (4−5), 237–246.

(26) Higuchi, T. Physical Chemical Analysis of Percutaneous Absorption Process from Creams and Ointments. *J. Soc. Cosmet. Chem.* **1960**, *11*, 85–97.

(27) Levich, V. G. *Physico-chemical hydrodynamics*; Prentice-Hall: Englewood Cliffs, NJ, 1962; pp 39−72.

(28) Kim, J. S.; Mitchell, S.; Kijek, P.; Tsume, Y.; Hilfinger, J.; Amidon, G. L. The suitability of an in-situ perfusion model for permeability determinations: utility for BCS class I biowaiver requests. *Mol. Pharmaceutics* **2006**, *3* (6), 686–694.

(29) Dahan, A.; Amidon, G. L. Segmental dependent transport of low permeability compounds along the small intestine due to P-glycoprotein: The role of efflux transport in the oral absorption of BCS class III drugs. *Mol. Pharmaceutics* **2009**, *6* (1), 19–28.

(30) Dahan, A.; Miller, J. M.; Hilfinger, J. M.; Yamashita, S.; Yu, L. X.; Lennernas, H.; Amidon, G. L. High-permeability criterion for BCS classification: Segmental/pH dependent permeability considerations. *Mol. Pharmaceutics* **2010**, *7* (5), 1827–1834.

(31) Fagerholm, U.; Johansson, M.; Lennernas, H. Comparison between permeability coefficients in rat and human jejunum. *Pharm. Res.* **1996**, *13*, 1336–1342.

(32) Dahan, A.; Sabit, H.; Amidon, G. L. Multiple efflux pumps are involved in the transepithelial transport of colchicine: Combined effect of p-glycoprotein and multidrug resistance-associated protein 2 leads to decreased intestinal absorption throughout the entire small intestine. *Drug Metab. Dispos.* **2009**, *37* (10), 2028–2036.

(33) Komiya, I.; Park, J. Y.; Kamani, A.; Ho, N. F. H.; Higuchi, W. I. Quantitative Mechanistic Studies in Simultaneous Fluid Flow and Intestinal Absorption Using Steroids as Model Solutes. *Int. J. Pharm.* **1980**, *4*, 249–262.

(34) Johnson, D. A.; Amidon, G. L. Determination of Intrinsic Membrane Transport Parameters from Perfused Intestine Experiments: A Boundary Layer Approach to Estimating the Aqueous and Unbiased Membrane Permeabilities. *J. Theor. Biol.* **1988**, *131*, 93–106.

(35) Dahan, A.; Hoffman, A. Use of a dynamic in vitro lipolysis model to rationalize oral formulation development for poor water soluble drugs: correlation with in vivo data and the relationship to intra-enterocyte processes in rats. *Pharm. Res.* **2006**, *23* (9), 2165–2174.

(36) Mudie, D. M.; Amidon, G. L.; Amidon, G. E. Physiological parameters for oral delivery and in vitro testing. *Mol. Pharmaceutics* **2010**, *7* (5), 1388–1405.